Role of Base Stacking and Sequence Context in the Inhibition of Yeast DNA Polymerase η by Pyrene Nucleotide†

Hanshin Hwang and John-Stephen Taylor*

Department of Chemistry, Washington University, St. Louis, Missouri 63130

Received May 23, 2004; Revised Manuscript Received August 11, 2004

ABSTRACT: The Y family DNA polymerase yeast pol η inserts pyrene deoxyribose monophosphate (dPMP) in preference to A opposite an abasic site, the 3′-T of a thymine dimer, and a normal T with almost equal efficiency. In contrast, pol A family polymerases such as Klenow fragment and T7 DNA polymerase only insert dPMP efficiently opposite an abasic site and the 3′-T of a thymine dimer but not opposite undamaged DNA. Pyrene nucleotide is also an efficient chain-terminating inhibitor of DNA synthesis by pol η but not by Klenow fragment or T7 DNA polymerase. To better understand the origin of the efficiency and sequence specificity of dPMP insertion by pol η, the kinetics of dPMP insertion opposite various templates have been determined. In one sequence context, the efficiency of dPMP insertion increases 4.6-fold opposite G < A ≪ T < C, suggesting that the templating nucleotide modulates dPMP insertion efficiency by having to destack prior to dPTP binding. The efficiency of insertion of dPMP opposite T in the same sequence context increases 7-fold for primers terminating in G < A < C < T and is similar to that observed for nontemplated blunt-end extension, suggesting that stacking interactions between the pyrene and the primer terminus are also important. On heterogeneous templates, the average selectivity for dPMP insertion relative to the complementary dNMP decreases in the order of dAMP > dGMP > dTMP > dCMP, from a high of 5.8 when dAMP is to be inserted following a T to a low of 0.5 when dCMP is to be inserted following a C. The relative preference for dPMP insertion at a given site can be largely explained by the energetic cost of destacking the templating base and stacking of pyrene nucleotide relative to that of stacking and base pairing the complementary nucleotide. Thus, pyrene nucleotide represents a novel class of nucleotide-based chain-terminating DNA synthesis inhibitors whose base portion consists of a hydrophobic, non-hydrogen bonding, base-pair mimic.

Yeast polymerase η (pol η)[1] (Rad30) is one of the newly discovered DNA damage bypass polymerases of the UmuC/DinB/Rev1/RAD30 superfamily of DNA polymerases (*1*−*6*) and is especially well-known for its ability to bypass the *cis-syn* thymine dimer efficiently and relatively non-mutagenically (*7*, *8*). The ability of pol η to bypass the *cis-syn* thymine dimer as well as other types of damage is ascribed to its relaxed requirement for correct base-pairing geometry at the active site in comparison to high-fidelity replicative polymerases, which require strict geometrical complementarity (*9*−*12*). Despite its ability to efficiently bypass a thymine dimer, pol η is about 1000 times less efficient at inserting opposite or extending past an abasic site than opposite a normal base and shows a preference for inserting purine over pyrimidine nucleotides opposite such a site (*13*).

Replicative DNA polymerases, such as Klenow fragment of *Escherichia coli* DNA polymerase I and T7 DNA polymerase, are also unable to efficiently bypass abasic sites and when they do, preferentially insert A (*14*−*16*), an observation which formed the basis of the "A-rule" (*17*, *18*). The preference for inserting A opposite an abasic site has been ascribed to its better base-stacking ability compared to the other three naturally occurring nucleotides (*15*). Recently, it was discovered that pyrene nucleotide, a nucleotide analogue whose base portion consists of a large flat aromatic molecule about the size of a base pair, is inserted opposite abasic sites with a greater preference than A by Klenow fragment, while it is not inserted opposite normal DNA bases (*19*). The preferential insertion of a pyrene nucleotide opposite an abasic site by Klenow fragment but not opposite a normal base supports the idea that base stacking and geometrical complementarity are very important for the action of this class of polymerases. Because pyrene nucleotide can only be inserted when the template strand lacks a base, it could be used to demonstrate that a *cis-syn* thymine dimer had to be outside the active site of T7 DNA polymerase during insertion opposite the 3′-T but not opposite the 5′-T (*20*).

When trying to use pyrene nucleotide to probe whether a thymine dimer was inside or outside the active site of yeast pol η, we discovered that pyrene nucleotide is not only preferentially inserted relative to dAMP opposite an abasic site and the 3′-T of a *cis-syn* thymine dimer, but also opposite a normal T (*21*). We also found that pyrene nucleotide was an efficient chain-terminating inhibitor of DNA synthesis by pol η but not by the Klenow fragment. We interpreted these

† This work was supported by NIH Grant CA40463.

* To whom correspondence should be addressed: Department of Chemistry, Campus Box 1134, Washington University, One Brookings Drive, St. Louis, MO 63130. Phone: (314) 935-6721. Fax: (314) 935-4481. E-mail: taylor@wustl.edu.

[1] Abbreviations: dPTP, pyrene deoxynucleotide triphosphate; pol η, polymerase η.

10.1021/bi0489558 CCC: $27.50
Published on Web 10/27/2004

results to suggest that pol η holds the templating nucleotide loosely, which makes it easy for pyrene deoxynucleotide triphosphate (dPTP) to displace the templating base and bind tightly to the active site by way of base-stacking interactions with the primer/template and hydrophobic interactions with the enzyme. We also suggested that these interactions might trigger the putative conformational change necessary to trigger phosphodiester bond formation by pol η. In support of a template base displacement mechanism, we found that pol η cannot insert pyrene nucleotide opposite the 5′-T of a dimer, which cannot be displaced because it is covalently linked to the 3′-T, which is presumably held tightly by the enzyme. In this paper, we use steady-state and pre-steady-state kinetic methods to investigate the mechanism of dPMP insertion opposite T, the 3′-T of a thymine dimer, and opposite an abasic site. We also investigate the effect of the templating nucleotide and the primer terminus on the efficiency and selectivity of dPMP insertion on undamaged templates in the presence of competing nucleotides and propose a mechanism for the inhibition of pol η by pyrene nucleotide.

MATERIALS AND METHODS

Enzymes and Substrates. The catalytic core of yeast pol η with a His_6 tag on its N terminus was prepared as previously described (*22*). Standard oligodeoxynucleotides and oligodeoxynucleotides containing an abasic site analogue were purchased from IDT and then purified by PAGE purification. Oligodeoxynucleotides containing a site-specific thymine dimer were synthesized on an Expedite 8909 DNA synthesizer utilizing a thymine dimer phosphoramidite building block (*23*, *24*) and then purified on an anion exchange DEAE column and on a C18 column. All DNA primers and templates used in this study are shown in Figure 1B. T4 polynucleotide kinase and [γ-^{32}P]ATP were obtained from Amersham Pharmacia Biotech. dPTP was prepared as previously described (*19*, *25*). Primers were labeled with [γ-^{32}P]ATP and polynucleotide kinase and were annealed with 1.25 equiv of templates by heating at 95 °C for 5 min and cooling over several hours.

Kinetic Experiments. Unless otherwise noted, all reactions were carried out in a reaction buffer containing 40 mM Tris-HCl at pH 7.5, 5 mM $MgCl_2$, 1 mM DTT, 10 μg/mL BSA, and 10% glycerol. Steady-state single nucleotide insertion reactions were carried out on large excess primer/template to pol η for the designated time at room temperature (RT) (temperature controlled at 23 °C) using various concentrations of deoxynucleotide triphosphates in 10 μL total volume. In steady-state direct competition assays, primer/templates were incubated with a mixture of competing nucleotides and pol η was added to initiate the reaction. The selectivity was then obtained as the slope of a linear least-squares fit of a plot of the ratio of products resulting from initial elongation of the 14-mer primer with each nucleotide as a function of the ratio of the two nucleotides as described before (*20*), using the equation in Figure 1D. For pre-steady-state experiments, preincubated pol η and primer/template were mixed with dNTP and then quenched at the designated time. To determine K_D^{dNTP} and k_{pol} in a single-turnover condition, preincubated pol η and primer/templates were mixed with dNTP and quenched at the designated time by addition of EDTA. Pre-steady state experiments were carried out on a BioLogic QFM-400 (Molecular Kinetics, Inc.) rapid mixing quench flow instrument that consists of four independently computer-controlled stepper motors that drive four syringes. This instrument is capable of delivering sample volumes as low as 10 μL and quenching in as short a time as 2 ms. Preincubation of the primer/templates with polymerases was carried out in the reaction buffer for a minimum of 5 min at RT. The quenched reaction mixtures were electrophoresed on a high-resolution denaturing 15% polyacrylamide gel and scanned by a BioRad Phosphorimager. The scanned bands were quantified by the volume integration methods using Quantity One software (BioRad).

Simulating and Fitting the Kinetic Data. To determine Michaelis−Menten parameters k_{cat} and K_m from steady-state single nucleotide insertion experiments, the initial insertion velocities were plotted as a function of the nucleotide concentration and fit to the Michaelis−Menten equation, $k_{obs} = (k_{cat}[dNTP])/(K_m + [dNTP])$. Under single-turnover conditions, the amount of product formed was plotted as a function of time and fit to the simple exponential rise equation, $[product] = [E](1 - e^{-kt})$, where k is the burst rate constant. To determine the k_{pol} and K_D^{dNTP} parameters for correct nucleotide insertion (dATP), the rate constants (k_{obs}) for nucleotide insertion were plotted as a function of the nucleotide concentration ([dNTP]) and fit to the hyperbolic equation, $k_{obs} = (k_{pol}[dNTP])/(K_D^{dNTP} + [dNTP])$. The data were fit by nonlinear least squares regression analysis with the Scientist version 2.01 software, and all equations used for fitting were shown in Figure 1C.

A)

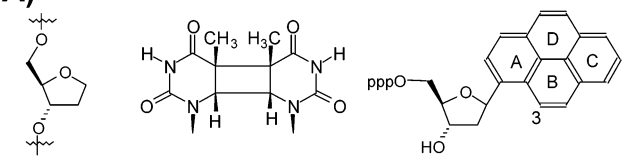

B)

```
14                    5'–AGATCGCAACTCAT – 3'
15X                   5'–AGATCGCAACTCATX – 3'
26  5'–GACTCAGCAGCTAGATCGCAACTCAT – 3'

50Y 3'–CTGAGTCGTCGATCTAGCGTTGAGTAY TATGAGCGTCACAGAAGTATCTA–5'
30D 3'–CTGAGTCGTCGATCTAGCGTTGAGTAT=TAT–5'
50ϕ 3'–CTGAGTCGTCGATCTAGCGTTGAGTAϕ TATGAGCGTCACAGAAGTATCTA–5'
                X or Y = A, C, G or T, D = dimer, ϕ = abasic site analog.
```

C)

(1) $[Product] = [E]*k_{obs}*t$

(2) $k_{obs} = k_{cat}*[N]/(K_m+[N])$

(3) $[Product] = [E]*(1-\exp(-k_{obs}*t))$

(4) $k_{obs} = k_{pol}*[N]/(K_D^{dNTP}+[N])$

D)

$$S_{P/N} = \frac{(k_{cat}/K_m)_{dPTP}}{(k_{cat}/K_m)_{dNTP}} = \frac{[14P]}{[14N + 14NP + 14NNP\ldots]} \bullet \frac{[dNTP]}{[dPTP]}$$

FIGURE 1: DNA substrates and the equations used to fit the data. (A) Structures of the abasic site analogue, *cis-syn* thymine dimer, and dPTP. The position on the pyrene nucleotide marked 3 corresponds to the 3 position in purine nucleotides. (B) DNA primers and templates used in this study. (C) Equations used to fit the steady-state and pre-steady-state kinetic data. (D) Equation for calculating the selectivity from direct competition experiments.

Table 1: Kinetic Parameters for Insertion of dAMP and dPMP by Yeast pol η Opposite the 3′-T of a TT Site or a *Cis-Syn* Thymine Dimer and an Abasic Site Analogue

```
26    5'-GACTCAGCAGCTAGATCGCAACTCAT
50T   3'-CTGAGTCGTCGATCTAGCGTTGAGTAT TATGAGCGTCACAGAAGTATCTA
30D   3'-CTGAGTCGTCGATCTAGCGTTGAGTAT=TAT
50ϕ   3'-CTGAGTCGTCGATCTAGCGTTGAGTAϕ TATGAGCGTCACAGAAGTATCTA
```

template	dNTP	$k_{cat} \pm$ SD (s^{-1})	$K_m \pm$ SD (μM)	k_{cat}/K_m ($\mu M^{-1}\ s^{-1}$)	$S_{P/A}$[a]
50T	dPTP	0.55 ± 0.01	0.55 ± 0.04	1.0	9.1
	dATP	0.20 ± 0.01	1.8 ± 0.2	0.11	
30D	dPTP	0.59 ± 0.02	0.58 ± 0.06	1.0	170
	dATP	0.11 ± 0.01	19 ± 2	0.0058	
50ϕ	dPTP	0.84 ± 0.02	0.59 ± 0.04	1.4	3800
	dATP	0.046 ± 0.002	126 ± 15	0.00036	
template	dNTP	$k_{pol} \pm$ SD (s^{-1})	$K_D \pm$ SD (μM)	k_{pol}/K_D ($\mu M^{-1}\ s^{-1}$)	$S_{P/A}$[a]
50T	dPTP	1.2 ± 0.1	1.3 ± 0.4	0.92	2.7
	dATP	2.5 ± 0.1	7.4 ± 0.6	0.34	
30D	dPTP	1.8 ± 0.2	1.6 ± 0.4	1.1	85
	dATP	0.28 ± 0.01	22 ± 2	0.013	
50ϕ	dPTP	1.1 ± 0.2	0.95 ± 0.45	1.2	750
	dATP	0.18 ± 0.01	113 ± 19	0.0016	

[a] Calculated as $(k_{cat}/K_m)_{dPTP}/(k_{cat}/K_m)_{dATP}$.

Continuous Extension Experiments. Continuous extension experiments were carried out by adding all four natural dNTPs and dPTP to 100 nM of pol η preincubated with 200 nM of primer/template and then quenched after incubating for the designated time at RT. The ratio of the amount of primer terminated by dPMP to that of primer extended by the complementary nucleotide gave the selectivity of dPMP insertion according to the equation shown in Figure 5B.

RESULTS

In a recent study, we found that pyrene nucleotide was preferentially and efficiently inserted opposite various template nucleotides, irrespective of their structure (*21*). To further investigate the molecular basis for the preferential insertion of pyrene nucleotide, steady-state and pre-steady-state kinetic measurements of nucleotide insertion opposite T, the 3′-T of the *cis-syn* thymine dimer, an abasic site model, and undamaged nucleotides were carried out. The structures of the abasic (apurinic/apyrimidinic) model, the *cis-syn* thymine dimer, and the pyrene deoxynucleotide triphosphate are shown in Figure 1A. The DNA substrates used in this study and the kinetic equations used to fit the data are shown in parts B and C of Figure 1.

Steady-State and Pre-Steady-State Kinetics of dPTP Insertion Opposite T, an Abasic Site, and a Thymine Dimer. Under steady-state conditions, the k_{cat} values for dPMP insertion opposite T, the 3′-T of the *cis-syn* thymine dimer, and an abasic site model varied only by 1.6-fold, while the K_m values hardly varied at all, resulting in efficiencies of about 1.0−1.4 $\mu M^{-1}\ s^{-1}$ (Figure 2 and Table 1). The small variation in these steady-state parameters indicates that the templating nucleotide has only a small influence on the insertion efficiency of dPMP. This is in sharp contrast to the insertion efficiency of dAMP, which was very sensitive to the nature of the templating base and dropped 18-fold on going from a normal T to the 3′-T of a *cis-syn* dimer and 300-fold to an abasic site. The decrease in efficiency is mainly due to large increases in K_m and to a lesser extent to small decreases in k_{cat}. Thus, the 9.1-, 170-, and 3800-fold increase in preference for dPMP compared to dAMP for insertion opposite T, the 3′-T of a dimer, and an abasic site, respectively, under steady-state conditions results exclusively from the decreased efficiency of dAMP insertion.

The maximum polymerization rates (k_{pol}) and the dissociation constants (K_D) for dPMP and dAMP insertion were determined from pre-steady-state kinetic experiments under single-turnover conditions and parallel the steady-state k_{cat} and K_m values (Figure 3 and Table 1). Both the k_{pol} and K_D values only varied by 1.5-fold for dPMP insertion opposite T, the 3′-T of the *cis-syn* thymine dimer, and the abasic site leading to similar insertion efficiencies of about 1 $\mu M^{-1}\ s^{-1}$. In contrast, the k_{pol} and K_D values for dAMP insertion were very sensitive to the nature of the templating nucleotide and varied more than 14-fold for k_{pol} and 18-fold for K_D. As a result, the efficiency of inserting dAMP dropped 26-fold on going from a normal T to the 3′-T of a thymine dimer and about 200-fold to an abasic site, which explains the 2.7-, 85-, and 750-fold drop in efficiencies compared to those for dPMP.

Effect of the Templating Base on dPMP Insertion Efficiency. In a previous study, we observed that synthesis by pol η opposite normal DNA in the presence of all four natural nucleotides was inhibited by pyrene nucleotide, which caused the formation of termination products with altered mobility (*21*). The formation of such termination products could be explained by competitive insertion and chain termination of synthesis by pyrene nucleotide, and in data not shown in that paper, it appeared that the sites of termination occurred with some sequence specificity. The formation of sequence-specific termination products would suggest that the sequence affects the efficiency of insertion of dPMP and/or the competing nucleotide or possibly the ability to extend pyrene nucleotide once inserted. The latter possibility is not likely to be of any significance because we have found very little evidence that primers terminating in pyrene nucleotide can be extended by pol η (vide infra). To sort out the first two possibilities, we first examined the effect of changing the templating nucleotide from T to A, C, and G on the insertion efficiency of dPMP and the complementary nucleotide (Table 2). In this situation, the contribution of base stacking of the

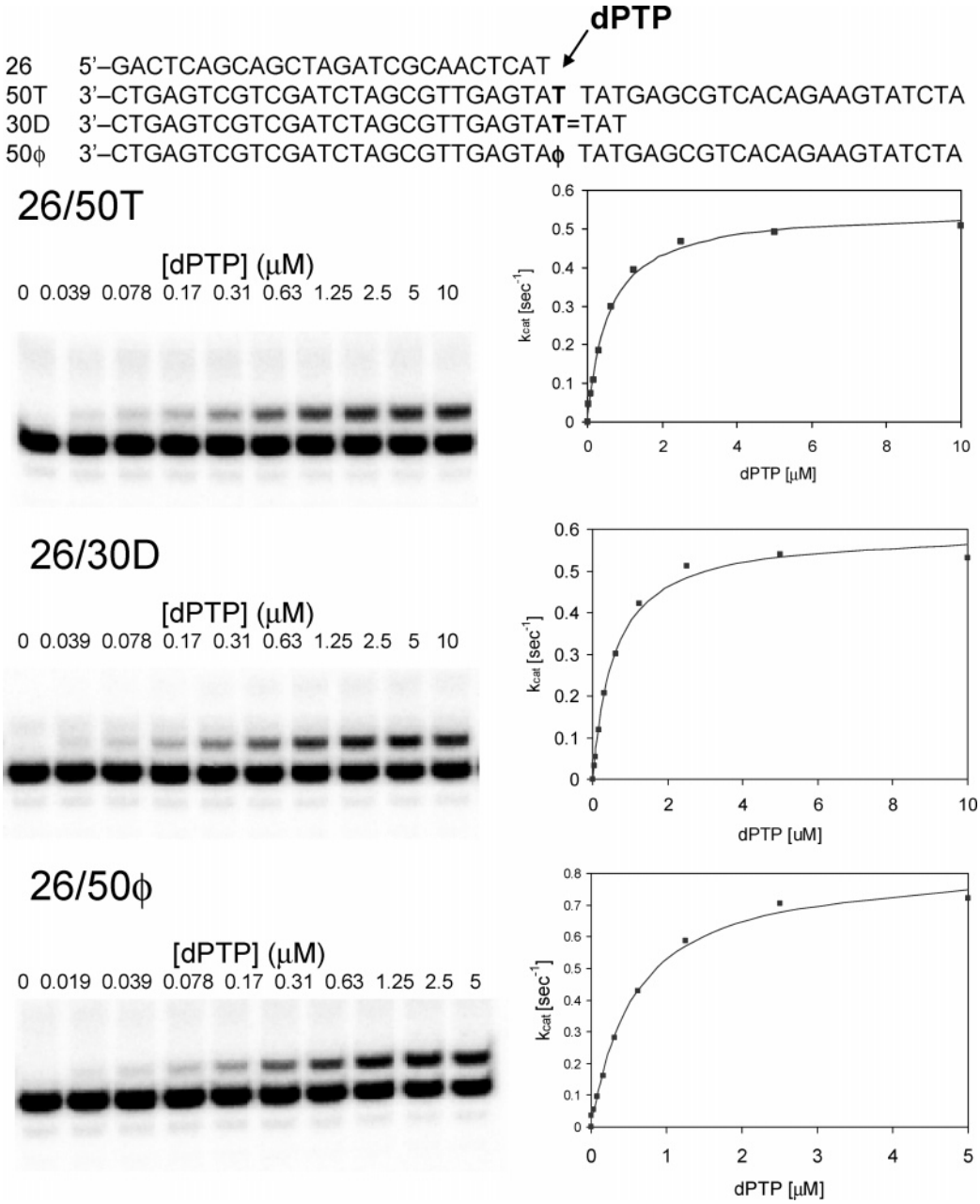

FIGURE 2: Insertion of dPMP opposite the 3′-T of TT and the *cis-syn* TT dimer and opposite the abasic site under steady-state conditions. pol η (0.5 nM) and excess primer/template (200 nM) were preincubated and then mixed with dPTP (0−10 μM) to initiate the reaction and quenched after 180 s with EDTA (100 mM) (all concentrations are final reaction concentrations). The solid line represents the best fit of the 27-mer product bands (■) resulting from extension of the 26-mer primer, according to the Michaelis−Menten kinetic model.

pyrene on the primer terminus to the efficiency of dPMP insertion would be the same for all templating bases, allowing the contribution from the templating base to be determined. The k_{cat} values decreased about 3-fold for dPMP insertion opposite C > T ≈ A > G, whereas the K_m values increased about 2.6-fold opposite T < C < A ≈ G. As a result, the steady-state efficiencies (k_{cat}/K_m) decreased about 4.6-fold for dPMP insertion opposite C > T ≫ A > G. The k_{cat} values for insertion of the complementary nucleotide decreased about 3-fold opposite G > C > A > T, whereas the K_m values increased about 2-fold opposite G ≈ T ≈ C < A. The net result was that the steady-state efficiencies for insertion of the complementary nucleotide decreased about 3-fold opposite G ≈ C > A ≈ T. The selectivity of dPMP insertion versus the correct nucleotide could be calculated from the ratio of the efficiencies, $(k_{cat}/K_m)_P/(k_{cat}/K_m)_N$, and decreased 12-fold opposite T ≫ C > A ≫ G. The selectivities were also independently determined from direct competition assays between dPTP and the complementary nucleotides and found to be very similar to those calculated from the single nucleotide experiments (Figure 4). Thus, dPMP competed better than the complementary nucleotide with decreasing selectivity opposite T > A ≈ C, whereas dCMP competed more efficiently than dPMP for insertion opposite G.

Effect of the Flanking Sequence on dPMP Insertion Efficiency. Because stacking of the templating base on the primer terminus was found to affect the efficiency of dPMP insertion, we then investigated the efficiency of dPMP and dAMP insertion opposite a template T as a function of

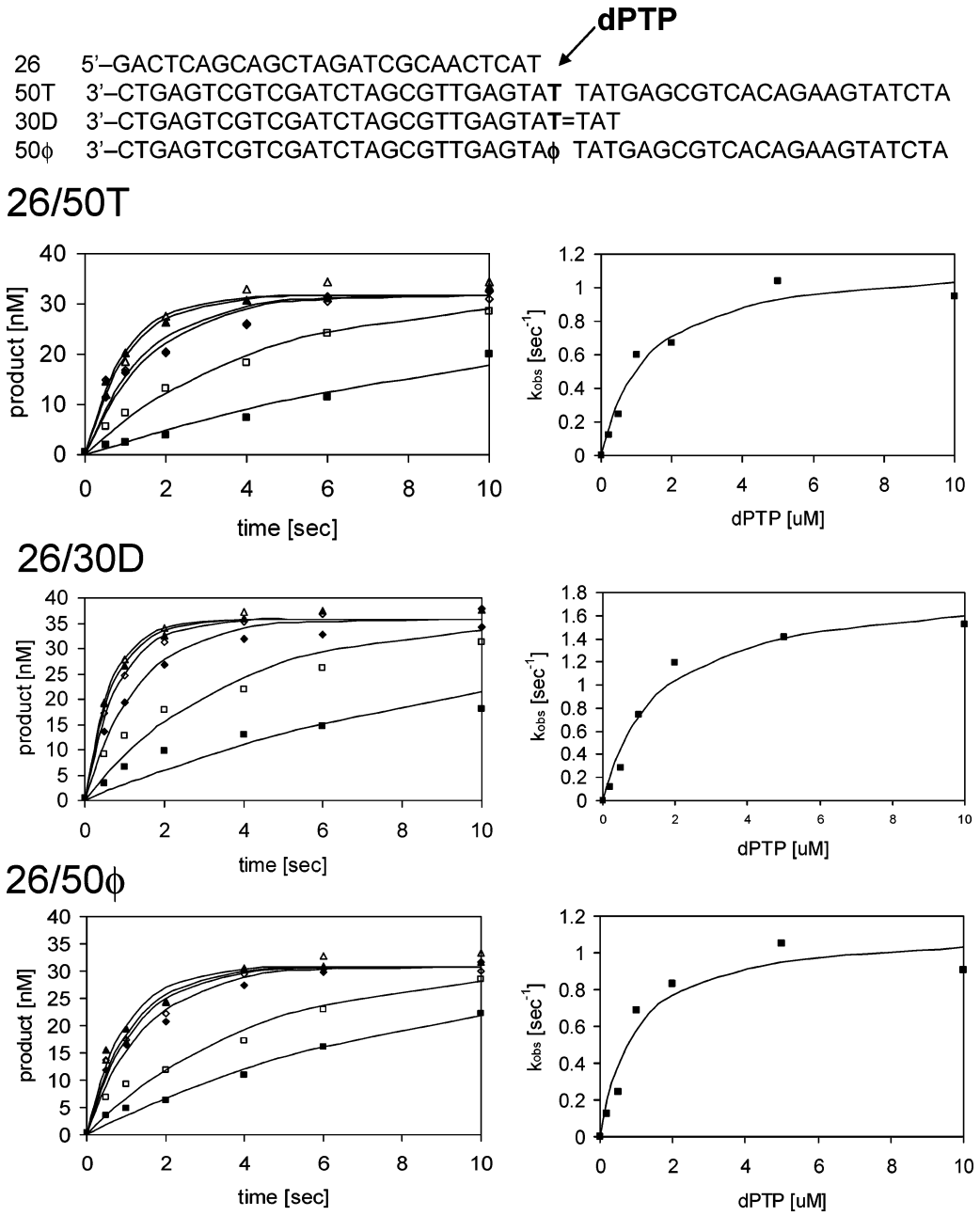

FIGURE 3: Insertion of dPMP opposite the 3′-T of TT and the *cis-syn* TT dimer and opposite the abasic site under single-turnover pre-steady-state conditions (excess enzyme over DNA template). Excess pol η (250 nM) was preincubated with primer/template (40 nM), then mixed with various concentrations of dPTP (■ for 0.2 μM, □ for 0.5 μM, ◇ for 1 μM, ◆ for 2 μM, ▲ for 5 μM, and △ for 10 μM) to initiate the reaction (final reaction concentrations), and quenched after the designated time with EDTA (100 mM). The solid lines represent the best fit of the extended product bands resulting from extension of the 26-mer primer, according to the simple exponential rise equation, eq 3, Figure 1C. Then, the calculated k_{obs} values are used to determine the k_{pol} and K_D^{dPTP} values according to the hyperbolic eq 4, Figure 1C.

different primer termini by steady-state single nucleotide insertion experiments (Table 3). In this case, base stacking of both the template T and the dNTP was expected to vary according to the base at the primer terminus. The k_{cat} values for dPMP insertion decreased almost 5-fold for extending T $\approx$ C > A $\approx$ G, while the K_m values only increased about 2-fold for extending A < T < C $\approx$ G. The net result was that the efficiencies for inserting dPMP opposite T decreased about 7-fold when extending T > C > A > G. In comparison, the k_{cat} values for insertion of dAMP decreased 2-fold when extending G $\approx$ A $\approx$ C > T, whereas the K_m values increased about 2-fold when extending T $\approx$ C $\approx$ A < G, resulting in efficiencies that decreased almost 2-fold for extending C $\approx$ A > T = G. Thus, the overall selectivity of dPMP insertion opposite T relative to A decreased almost 7-fold when extending from T > C > A > G, demonstrating that flanking sequence has a substantial affect on the selectivity of pyrene nucleotide insertion opposite T.

Because the effect of the base pair at the primer terminus on dPMP could not be separated from its effect on the templating nucleotide, blunt-end primer/templates were investigated, which eliminate the contribution from the templating nucleotide. (Table 4). Although the absence of a templating nucleotide dramatically reduced k_{cat}, the effect of the primer terminus on pyrene nucleotide insertion could be readily discerned. The k_{cat} values decreased 11-fold for

Table 2: Steady-State Kinetic Parameters for Insertion of the Correct Nucleotide and Pyrene Nucleotide by Yeast pol η Opposite A, C, G, and T

```
14          5'-AGATCGCAACTCAT
50Y  CTGAGTCGTCGATCTAGCGTTGAGTAYTATGAGCGTCACAGAAGTATCTA
```

template Y	dNTP	$k_{cat} \pm$ SD (s^{-1})	$K_m \pm$ SD (μM)	k_{cat}/K_m (μM^{-1} s^{-1})	$S_{P/N}$[a]	$S_{P/N}$[b] (from competition assay)
T	dPTP	0.33 ± 0.02	0.58 ± 0.13	0.57	8.5	9.4
	dATP	0.32 ± 0.01	4.8 ± 0.5	0.067		
C	dPTP	0.61 ± 0.04	0.94 ± 0.23	0.65	4.3	3.3
	dGTP	0.75 ± 0.02	5.0 ± 0.4	0.15		
A	dPTP	0.31 ± 0.02	1.33 ± 0.25	0.23	3.4	3.4
	dTTP	0.65 ± 0.04	9.5 ± 1.4	0.068		
G	dPTP	0.21 ± 0.01	1.5 ± 0.32	0.14	0.71	0.59
	dCTP	0.90 ± 0.04	4.6 ± 0.7	0.20		

[a] Calculated as $(k_{cat}/K_m)_{dPTP}/(k_{cat}/K_m)_{dNTP}$. [b] As defined in Figure 1D.

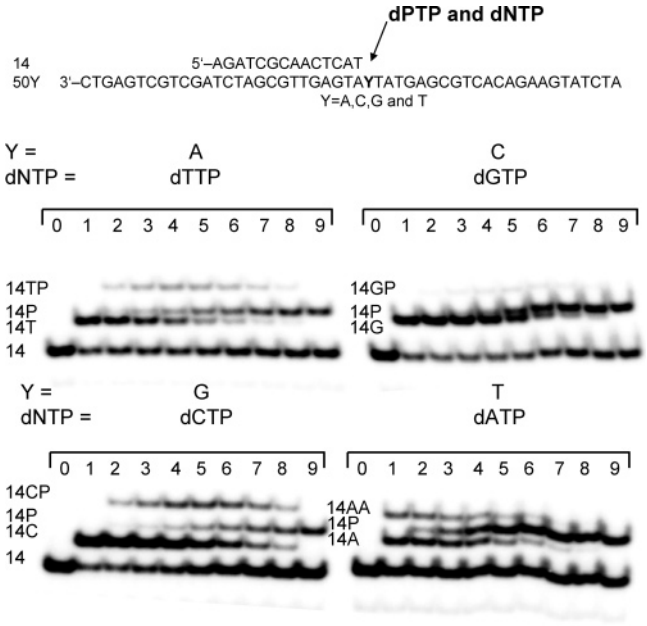

FIGURE 4: Direct competition assay between inserting dPMP versus the complementary nucleotide opposite the normal DNA template. pol η (1 nM) was incubated with excess primer/template (200 nM), then mixed with dPTP and the complementary nucleotide at a total concentration of 20 μM, and quenched after 120 s with EDTA (100 mM). Lanes 1−9 correspond to dPTP/dNTP ratios of 0:100, 2:98, 5:95, 10:90, 20:80, 30:70, 50:50, 70:30, and 100:0, respectively. The ratio of dPMP extended product and dNTP extended products were used to calculate the selectivity according to the equation in Figure 1D.

extending T > C > A > G, and the K_m values increased almost 2-fold for extending A = T < C < G. The net efficiencies decreased about 5-fold for extending T > C > A > G with pyrene nucleotide. Thus, the order of insertion efficiency was the same as in the presence of a templating T, but the magnitude of the efficiency decreased about 160-fold for extending A, 78-fold for C, 220-fold for G, and 85-fold for T.

Continuous Extension Experiments. To investigate the effect of each possible combination of templating nucleotide and primer terminus on the efficiency of dPMP insertion by pol η would require 16 DNA primer/templates. Rather than determine the individual kinetic parameters for the insertion of dPMP and the complementary nucleotide at each site, we decided to construct single templates containing all 16 unique dinucleotide sequences and examined the relative efficiency of dPMP insertion at each site during continuous synthesis (Figure 5A). Four 50-mer templates were constructed, each containing the same 14-mer long primer-binding site, a 17-mer section containing a different arrangement of the 16 unique dinucleotide sequences, and a 5′-terminal A_6 tract. Figure 6 shows the autoradiogram of the PAGE gels of the products of primer extension on these templates with only dNTPs and with dNTPs in the presence of dPTP at two different time points. The pyrene-terminated products can be identified by their different mobility compared to products produced in the absence of dPTP, and the pattern of pyrene-terminated product bands is the same at 10 min as at 5 min, indicating that they cannot be further extended. The only band that clearly appears to decrease with time (5 min lane of Comb50C, Figure 6) can be attributed to a natural pause site terminating in a normal nucleotide by comparison to the lane which has no pyrene nucleotide. In only one case do we see a band that increases (20 min lane, Figure 5B) that might be attributable to further elongation of a pyrene-terminated primer. With this possible exception, primers terminating in dPMP did not appear to be further extended under the conditions used, and therefore, the selectivity for dPMP insertion relative to the complementary nucleotide could be calculated from the equation shown in Figure 5B. The dPMP insertion selectivities calculated in this way did not vary significantly with times from 5 to 20 min but did vary opposite the same dinucleotide sequence in different sequence contexts, indicating that sequence context beyond the primer terminus influences the insertion selectivity. In general, the selectivities obtained from single nucleotide insertion experiments were comparable to those obtained from the continuous extension experiments and are summarized in Table 5. Figure 7 shows the termination selectivities as a function sequence context in order of decreasing selectivity. As can be seen, termination selectivity generally decreased when the complementary nucleotide changed in the order of dATP > dGTP > dTTP > dCTP, with the greatest selectivity occurring when a dATP was to be inserted following a T and the lowest occurring when dCTP was to be inserted following a C.

DISCUSSION

dPTP Insertion Opposite an Abasic Site. Insertion of normal nucleotides opposite an abasic site is very inefficient for both A (*26*) and Y family polymerases (*13*). This may be attributable to the absence of a templating base that may be needed to trigger the rate-limiting conformational change that precedes phosphodiester bond formation (*27*−*29*). In contrast, dPMP is inserted opposite an abasic site by A family

Table 3: Effect of Primer Terminus on Steady-State Kinetic Parameters for Insertion of dATP and dPTP by Yeast pol η Opposite T

```
15X          5'-AGATCGCAACTCATX
50Y  CTGAGTCGTCGATCTAGCGTTGAGTAYTATGAGCGTCACAGAAGTATCTA
```

primer X	template Y	dNTP	$k_{cat} \pm$ SD (s^{-1})	$K_m \pm$ SD (μM)	k_{cat}/K_m ($\mu M^{-1}\ s^{-1}$)	$S_{P/N}$[a]
T	A	dPTP	0.39 ± 0.01	0.57 ± 0.10	0.68	17
		dATP	0.17 ± 0.01	4.3 ± 0.3	0.040	
C	G	dPTP	0.35 ± 0.02	0.76 ± 0.15	0.46	6.6
		dATP	0.31 ± 0.01	4.4 ± 0.1	0.070	
A	T	dPTP	0.12 ± 0.01	0.44 ± 0.08	0.27	4.4
		dATP	0.32 ± 0.01	5.2 ± 0.4	0.062	
G	C	dPTP	0.085 ± 0.004	0.87 ± 0.15	0.098	2.5
		dATP	0.37 ± 0.01	9.1 ± 0.6	0.040	

[a] Calculated as $(k_{cat}/K_m)_{dPTP}/(k_{cat}/K_m)_{dNTP}$.

Table 4: Effect of the Primer Terminus on the Steady-State Kinetic Parameters for Insertion of DPMP to a Blunt End by Yeast pol η

```
15X          5'-AGATCGCAACTCATX
27Y  CTGAGTCGTCGATCTAGCGTTGAGTAY
```

primer X	template Y	$k_{cat} \pm$ SD (s^{-1})	$K_m \pm$ SD (μM)	k_{cat}/K_m ($\mu M^{-1}\ s^{-1}$)	relative efficiency
T	A	0.0113 ± 0.0003	1.4 ± 0.1	0.0080	18
C	G	0.0099 ± 0.0002	1.7 ± 0.1	0.0059	13
A	T	0.0023 ± 0.0001	1.4 ± 0.1	0.0017	3.8
G	C	0.0010 ± 0.0001	2.3 ± 0.2	0.000 45	1

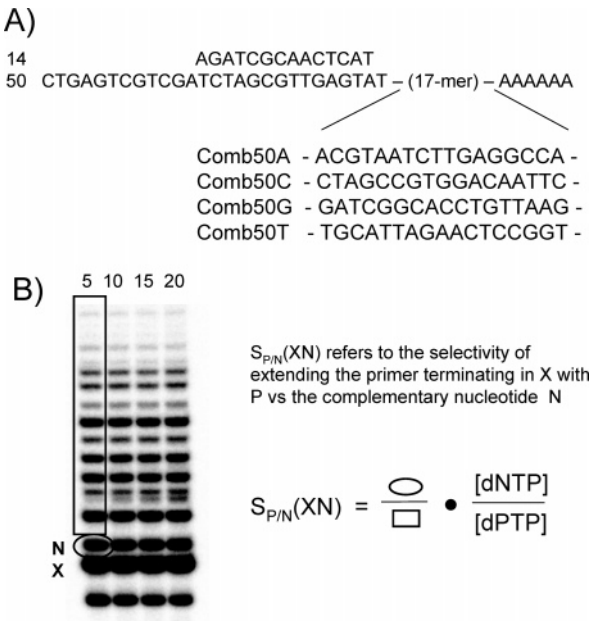

FIGURE 5: (A) DNA primers and templates used in continuous extension experiments. (B) Method to calculate the selectivity of pyrene nucleotide in continuous extension experiments, where ○ refers to the volume-integrated intensity of the band terminating in P and □ refers to the volume-integrated intensity of all of the following bands. Shown are the products of extension opposite Comb50A in the presence of dPTP and all dNTPs carried out under the conditions listed in Figure 6 for the times indicated in minutes.

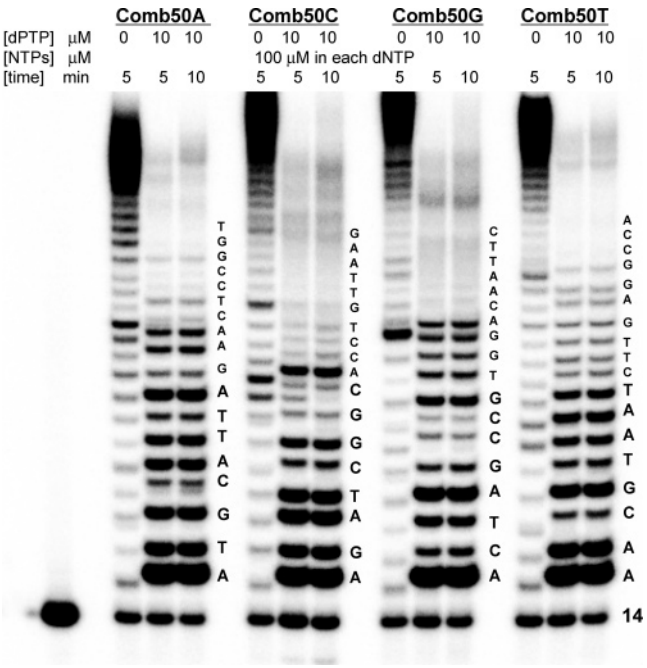

FIGURE 6: Continuous extension experiments. pol η (100 nM) was preincubated with the primer/template (200 nM), then mixed with 100 μM of all four natural dNTPs and either 0 or 10 μM dPTP (final reaction concentrations), and quenched after 5 or 10 min with EDTA (100 mM). The selectivities of pyrene nucleotide versus the correct nucleotide were calculated from the equation in Figure 5B. The sequence of the primer strand is shown alongside the corresponding bands.

polymerases almost as efficiently as is a normal nucleotide opposite a complementary base. In the case of the Klenow fragment of *E. coli* pol I, the steady-state efficiency of dPMP insertion opposite an abasic site is 300−2000-fold higher than for the insertion of a normal nucleotide (*19*). Our results show that pol η also inserts dPMP 3800-fold more efficiently than dATP opposite the abasic site under steady-state conditions and 750-fold more under pre-steady-state conditions with an efficiency that is comparable to that for inserting dAMP opposite T (Table 1). The high efficiency of dPMP insertion is all the more remarkable considering that 3-deazaguanosine monophosphate, which lacks an H-bond acceptor at the 3 position like pyrene nucleotide (Figure 1), is inserted 170-fold less efficiently than G opposite C (*30*). Clearly, any decrease in the efficiency of dPMP insertion because of the lack of an H-bond acceptor at the 3 position must be compensated for by other factors.

The preferential insertion of dAMP opposite an abasic site by many polymerases is the basis of the A-rule (*17*, *18*) and

Table 5: Specificity of DNA Synthesis Termination by Pyrene Nucleotide for All Possible Combinations of the Primer Terminus and Templating Base

primer terminus	dNTP	template base	Comb50A[a]	Comb50C[a]	Comb50G[a]	Comb50T[a]	average $S_{P/N} \pm$ SD	$S_{P/N}$[b]
T	A	T	6.37	nd[c]	5.13	nd	5.8 ± 0.9	8.5, 17
	G	C	2.50	nd	1.24	1.88	1.9 ± 0.6	4.3
	T	A	1.05	nd	nd	1.56	1.3 ± 0.4	3.4
	C	G	nd	1.11	nd	1.39	1.3 ± 0.2	0.71
A	A	T	4.21	nd	nd	3.77	4.0 ± 0.3	4.4
	G	C	1.43	1.84	0.95	nd	1.4 ± 0.4	
	T	A	2.21	4.34	nd	3.86	3.5 ± 1.1	
	C	G	1.53	0.88	0.73	0.66	1.0 ± 0.4	
G	A	T	3.17	3.96	2.96	nd	3.4 ± 0.5	2.5
	G	C	nd	0.70	2.05	nd	1.4 ± 1	
	T	A	nd	nd	1.50	1.18	1.3 ± 0.2	
	C	G	0.67	1.08	0.53	nd	0.8 ± 0.3	
C	A	T	2.16	4.15	nd	nd	3.2 ± 1.4	6.6
	G	C	nd	2.43	2.56	4.43	3.1 ± 1.1	
	T	A	nd	0.71	1.32	1.48	1.2 ± 0.4	
	C	G	nd	0.63	0.41	nd	0.52 ± 0.15	

[a] Average of 5 and 10 min data. [b] From Tables 2 and 3. [c] Could not be determined accurately because of the band smearing in the upper region of the gel.

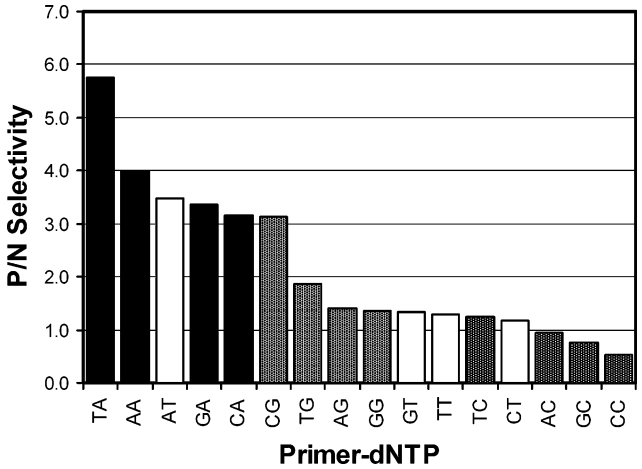

FIGURE 7: P/N termination selectivities extracted from the continuous extension experiments shown in Figure 6. The selectivities are shown in decreasing order for NN, where the first base is that of the primer terminus and the second is that of the incoming dNTP that is complementary to the templating base. The bars are colored according to the templating base, with black = T, white = A, light gray = C, and dark gray = G, showing that the magnitude of pyrene nucleotide insertion selectivity relative to the complementary dNTP depends primarily on the templating base and secondarily to the primer terminus.

has been suggested to arise from the greater hydrophobic stacking interactions between A and the 3′-terminal base pair of the primer than for other bases (*15*, *31*). pol η actually shows a slightly higher preference for inserting G than A opposite an abasic site, but both are more efficiently inserted than pyrimidines (*13*). Because pyrene is more hydrophobic than A and lacks H-bonding capability (*32*), the greater preference for insertion of dPMP than dAMP opposite an abasic site supports the rationale for the A-rule. Pyrene is about the same size as a Watson−Crick base pair that it stacks upon and thus has additional interstrand-stacking interactions with the base in the template that are not possible with A that can further stabilize the polymerase−DNA−dPTP complex. A duplex with a pyrene nucleotide opposite an abasic site has been found to be 5.1 kcal/mol more stable than the corresponding duplex with A opposite the abasic site (*33*). The increased capability of dPMP for interstrand base stacking compared to dAMP could explain in part why its insertion efficiency does not depend on the presence of a templating base, whereas it does for dAMP. The large size of pyrene can also presumably compensate for the absence of a template base and possibly restore binding to the polymerase and/or trigger the putative conformational change that precedes phosphodiester bond formation (*29*). The fact that pyrene nucleotide is able to trigger this conformational change is suggested by the high k_{pol} values for dPMP insertion opposite an abasic site obtained from pre-steady-state experiments (Table 1). The k_{pol} values are only slightly less than that for dAMP insertion opposite a normal T and are presumably limited by the rate of the conformational change that precedes phosphodiester bond formation.

dPTP Insertion Opposite the Cis-Syn Thymine Dimer. We had previously shown that the A family T7 DNA polymerase preferentially inserts pyrene nucleotide in preference to A opposite the 3′-T of a series of dithymidine photoproducts including the *cis*- and *trans-syn* cyclobutane dimers and the (6−4) and Dewar photoproducts but not opposite the 5′-T (*20*). This behavior was used to support a proposed mechanism for the dipyrimidine photoproduct bypass by A-family polymerases in which insertion opposite the 3′-pyrimidine of the photoproduct occurs with the photoproduct outside the active site, whereas insertion opposite the 5′-T occurs with the photoproduct inside the active site. This proposal was originally based on the crystal structure of T7 DNA polymerase complexed to a template primer and dNTP (*34*), which revealed that the active site was not big enough to accommodate a dithymidine photoproduct during insertion opposite the 3′-T but could accommodate it during insertion opposite the 5′-T. Hence, insertion opposite the 3′-T occurs via a transient abasic site-like intermediate in which pyrene insertion is preferred, whereas insertion opposite the 5′-T occurs with the dimer inside the active site, which prevents pyrene nucleotide from binding.

We also found that pol η behaves in a similar way to T7 DNA polymerase toward a *cis-syn* thymine dimer, preferentially inserting pyrene nucleotide relative to dAMP opposite the 3′-T but not opposite the 5′-T (*21*). Unlike T7 DNA polymerase, pol η can accommodate a thymine dimer in the active site during insertion opposite the 3′-T dimer, as revealed by the efficient insertion of dAMP opposite the

3′-T of the dimer, but not when base pairing is blocked by methylation of N3 of the 3′-T (*21*). For pyrene nucleotide to be inserted opposite the 3′-T of the dimer as efficiently as opposite an abasic site would require that the dimer be held very loosely and hence would be easily displaced from the active site. The conclusion that the dimer must be held rather loosely by pol η comes from the almost identical steady-state and pre-steady-state kinetic parameters for pyrene nucleotide insertion opposite an abasic site and the 3′-T of a thymine dimer (Table 1). Evidence that the templating base must be displaced from its normal position to accommodate pyrene nucleotide comes from the observation that pyrene nucleotide cannot be inserted opposite the 5′-T of the thymine dimer (*21*). In this case, the 5′-T is locked into the templating position by being covalently linked to the 3′-T, which must be held tightly by the polymerase so that the pyrene cannot displace the entire thymidine dimer from the active site. The inability to insert pyrene nucleotide opposite the 5′-T of the dimer helps rule out structures in which the pyrene ring sits on top or lies to the side of the templating base during insertion.

dPTP Insertion Opposite Normal T. In contrast to the otherwise similar behavior of T7 DNA polymerase and pol η with respect to preferentially inserting dPMP opposite an abasic site and the 3′-T of a thymine dimer, yeast pol η also efficiently inserts dPMP opposite a normal T, whereas T7 DNA polymerase does not. This difference is consistent with the idea that the active site of T7 DNA polymerase is so constrained that it cannot simultaneously accommodate both pyrene nucleotide and a templating base, whereas pol η can. Modeling studies of the crystal structure of the catalytic core of pol η (*35*) and of the crystal structure of a Dpo4, another Y family polymerase, complexed to a thymine dimer (*36*) suggest that pol η has a wide and open active site that can accommodate a thymine dimer. The active site appears open enough that it could readily accommodate pyrene nucleotide opposite a normal base by either having the base flipped out of the active site entirely or by having the templating base sit upon the pyrene ring in some fashion (an intercalated intermediate, Figure 8B). In either case, the templating base would have to destack to allow the pyrene nucleotide to stack upon the templating base.

The maximum polymerization rate constant (k_{pol}) and the dPTP binding affinities for the pol−DNA complex (K_D) for dPMP insertion opposite the abasic site, the normal T, and the 3′-T of the *cis-syn* dithymine dimer are almost the same, indicating that all of the templates behave like an abasic site. The similarity of the kinetic data support the idea that dPTP insertion opposite T and the 3′-T of a dimer occurs via a transient abasic site-like intermediate, in which the templating base is not stacked on the primer terminus during binding and insertion of the dPMP. It would appear that the lack of base pairing between the pyrene and the abasic-like template after displacement of the template base is more than compensated by the enhanced base-stacking interactions, which may even facilitate the dPMP insertion reaction. In fact, it has been found that duplexes containing pyrene opposite normal nucleotides are much less destabilized than duplexes containing smaller, non-H-bonding nucleotides (*33*). In this regard, it has been found that the smaller difluorotoluene nucleotide, a hydrophobic, non-H-bonding isostere of thymidine nucleotide, is 218 times less efficiently inserted

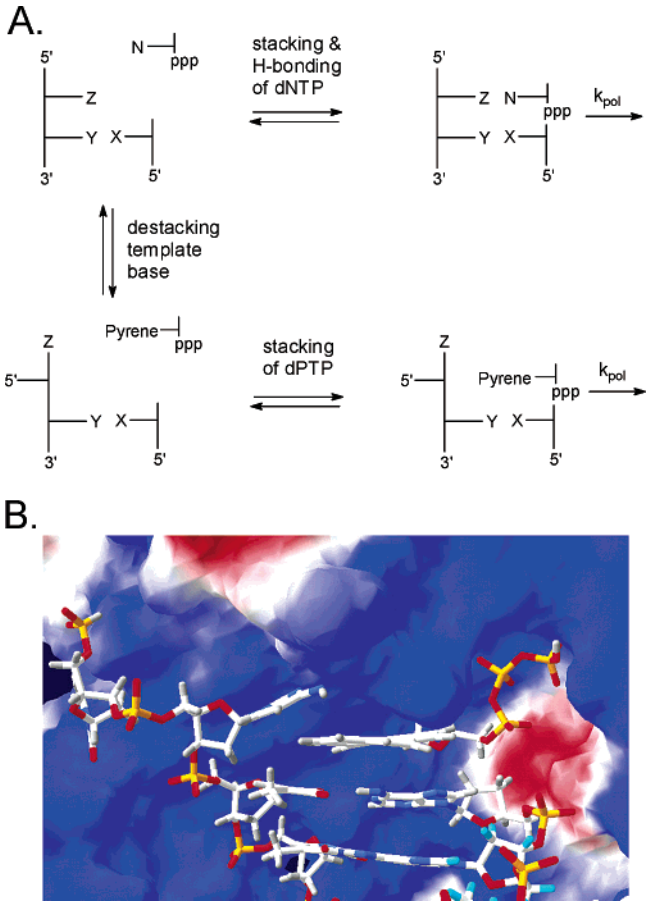

FIGURE 8: Template base displacement mechanism for the insertion of dPTP opposite undamaged DNA by pol η. (A) Basic kinetic scheme for the competitive insertion of dPMP versus a complementary nucleotide that involves destacking of the templating base to form a transient abasic site-like intermediate prior to binding of dPTP, which then triggers phosphodiester bond formation. It is also possible that the templating base is not completely displaced from the active site and that pyrene nucleotide intercalates in one step between the template bases as modeled in B. (B) Model of pol η bound to a DNA primer/template and dPTP showing how the large unconstrained active site can accommodate both pyrene nucleotide and the displaced templating base at the same time. The model was generated by Swiss-PDB viewer.

opposite A than T by pol η (*37*). When these results are taken all together, they emphasize the important role of interstrand base stacking in the efficient insertion of pyrene nucleotide by yeast pol η.

Effect of the Templating Base on Pyrene Nucleotide Insertion Efficiency. If the templating base has to destack to accommodate the pyrene nucleotide, one might expect that the efficiency of dPMP insertion would decrease as the stacking energy of the template base with the base pair at the primer terminus increases. One way to estimate the energetic cost of destacking the templating base is to consider the free energies for 5′-dangling bases in DNA and RNA. For DNA, the order of stability for a 5′-dangling base with A at the adjacent 3′ site is C < A < G < T (*38*), whereas for RNA the order is reported to be U < C = A < G (*39*). The efficiency of extending a primer terminating in T by dPMP varied 5-fold, decreased for insertion opposite C ≈ T > A > G (Table 2), and roughly paralleled the K_m values as would be expected if destacking of the templating base affected binding of dPTP. The observed order of pyrene

nucleotide insertion efficiency more closely matches the order predicted by the dangling RNA base energies, which would indicate that the template primer adopts more of an A conformation than a B conformation in the active site of pol η. The A conformation of template primers has been observed in the active sites of a number of other DNA polymerases including T7 DNA polymerase (*34*), Taq polymerase (*40*), and pol β (*41*).

The selectivities for dPMP insertion relative to the complementary dNMP vary about 15-fold and parallel the efficiencies for dPMP insertion, decreasing in the order opposite T > C ≈ A > G. The large variation in selectivity can be seen to arise from the 5-fold variation in efficiency of dPMP insertion coupled with an about 3-fold greater efficiency of forming a G·C base pair compared to an A·T base pair. It is interesting to note that we observe the efficiency of inserting dGMP opposite C or dCMP opposite G as about the same, and the same holds true for forming A·T base pairs, suggesting that base pairing (3 H bonds versus 2 H bonds) plays a more important role than base stacking in the insertion of normal nucleotides. These efficiencies are different, however, from those in a previous report in which the efficiency for inserting dNMP opposite the complementary base by pol η decreased in the order of dCMP > dTMP > dAMP > dGMP with relative efficiencies of 12:3.7:2.7:1 in a similar sequence context (*42*). In a different sequence context, the corresponding efficiencies were 4.3:1.8:1.2:1, although the K_m values reported differ from the other report by factors of up to 100 (*13*). It may be that the efficiency of forming GC base pairs is highly sequence-dependent.

Effect of the Primer Terminus on the Efficiency of Pyrene Nucleotide Insertion. Given that base stacking is largely responsible for the efficient insertion of pyrene nucleotide opposite both damaged and undamaged templates, one might also expect that the efficiency of dPMP insertion will also depend on the base pair at the primer terminus. With substrates in which the templating base was held constant, while the base at the primer terminus was varied, the efficiencies of dPMP insertion opposite a T varied 7-fold, whereas the efficiencies of dAMP insertion only varied 1.8-fold (Table 3). dPMP was inserted most efficiently when the terminal nucleotide was T and least when it was G, with an overall order of T > C > A > G. The same order of efficiency was observed with blunt-ended primer/templates, which lack a templating base, although the efficiencies were greatly reduced (Table 4). The greatly decreased efficiency for inserting dPMP at a blunt end is surprising, considering that it is very efficiently inserted opposite an abasic site, and suggests that the single-strand template plays an important role in anchoring and/or positioning the template primer. The order of efficiency in extending a blunt end by dPMP is similar to that of extending T > A > C > G (4.3:1.9:1.3:1) by dAMP opposite abasic sites by *Drosophila* DNA polymerase α (*15*). It was noted in that study that, because the 5′-TA-3′ doublet is thermodynamically less stable than 5′-AA-3′, 5′-CA-3′, and 5′-GA-3′ doublets, the greater efficiency for inserting A following a T might be due to the better stabilizing affect of interstrand A−A stacking than intrastrand T−A stacking.

When one considers all of the possible sequence contexts, the selectivity for pyrene nucleotide insertion seems to be more dependent on the nature of the templating base than on the primer terminus, decreasing as the templating base changes in the order of T > C > A > G (Figure 7). The dependence on the templating base suggests that destacking of the templating base plays a major role in determining the selectivity. For a given templating base, however, the average selectivity decreases as the primer terminus changes from T > A > G > C, except when the templating base is A or C. When the templating base is A, the T is out of order (A > G > T > C), and when the templating base is C, the C is out of order (C > T > A > G). The observed order is different than that of T > C > A > G for dPMP addition to the blunt-ended primer and may reflect an additional contribution from sequence-dependent destacking of the templating base. Although these appear to be general trends, the termination selectivities for a given primer terminus and templating base vary 2-fold or more (Table 5), indicating that more remote sequences also influence selectivity in some yet unknown way.

Termination of DNA Synthesis by dPMP Insertion. Although pyrene nucleotide is efficiently inserted by pol η irrespective of whether the template contains an abasic site, the 3′-T of a dimer, or a normal nucleotide, further extension is highly inefficient and was not observed under the conditions studied. The A family T7 DNA polymerase and the Klenow fragment also do not extend primers terminating pyrene opposite an abasic site (*19*) or the 3′-T of dithymidine photoproducts (*20*), but this may be largely due to the abasic or abasic-like site, because these polymerases also do not efficiently extend an A opposite an abasic site. The inability to extend pyrene nucleotide opposite normal bases may be due to distortion of the templating base and the template strand that results from having to stack the displaced base or the one to its 5′ side on top of the pyrene (Figure 8b). It is also possible that the primer terminus becomes distorted because of an inappropriate base-stacking geometry, due to steric interactions, or the inability to form H-bonding interactions between the minor groove side of the pyrene and the polymerase. H-bonding interactions between the nascent base pair and the amino acid residues of polymerase have been found to be important in DNA synthesis by a variety of polymerases (*34*, *43*, *44*), although it appears that the only H-bonding to the minor groove in pol η occurs at the nucleotide triphosphate-binding site (*30*). Examination of NMR-derived structures of pyrene nucleotide inserted opposite an abasic site in duplex DNA (Protein Data Bank structure 1FZL) clearly shows that the B ring (Figure 1) protrudes farther into the minor groove than would a normal base and might have bad steric interactions with the polymerase (*45*). Thus, it may not be possible for the pyrene nucleotide to adopt the appropriate geometry for phosphodiester bond formation.

CONCLUSION

We have shown that pyrene nucleotide, a nucleotide that lacks any H-bond donors or acceptors, is much more efficiently inserted by yeast pol η opposite normal bases than the complementary nucleotides in most sequence contexts. The high efficiency of dPMP insertion appears to be due in large part to strong base-stacking interactions between the pyrene ring and the primer terminus base pair. It is also possible that pyrene can trigger the conformational change

that is coupled to phosphodiester bond formation by virtue of its ability to subsume the role of the templating base. The sequence specificity of pyrene nucleotide insertion appears to be largely dominated by the templating base and secondarily to the primer terminus and can be explained by a mechanism in which the templating base must destack prior to stacking of pyrene nucleotide (Figure 8). Whether or not the pyrene intercalates between the template bases or the templating base is flipped outside of the active site is not known at the moment. Thus, pyrene nucleotide represents a new class of nucleotide-based chain-terminating DNA polymerase inhibitors whose base portion consists of a hydrophobic, non-hydrogen-bonding base-pair mimic. Pyrene nucleotide can serve as a prototype for the design of more efficient and selective inhibitors of pol η and perhaps other Y family polymerases, which could be used to suppress the mutagenic and carcinogenic bypass of DNA damage.

REFERENCES

1. Friedberg, E. C., and Gerlach, V. L. (1999) Novel DNA polymerases offer clues to the molecular basis of mutagenesis, *Cell 98*, 413−416.
2. Woodgate, R. (1999) A plethora of lesion-replicating DNA polymerases, *Genes Dev. 13*, 2191−2195.
3. Cordonnier, A. M., and Fuchs, R. P. (1999) Replication of damaged DNA: Molecular defect in xeroderma pigmentosum variant cells, *Mutat. Res. 435*, 111−119.
4. Goodman, M. F., and Tippin, B. (2000) The expanding polymerase universe, *Nat. Rev. Mol. Cell Biol. 1*, 101−109.
5. Livneh, Z. (2001) DNA damage control by novel DNA polymerases: Translesion replication and mutagenesis, *J. Biol. Chem. 276*, 25639−25642.
6. Wang, Z. (2001) Translesion synthesis by the UmuC family of DNA polymerases, *Mutat. Res. 486*, 59−70.
7. Johnson, R. E., Prakash, S., and Prakash, L. (1999) Efficient bypass of a thymine−thymine dimer by yeast DNA polymerase, pol η, *Science 283*, 1001−1004.
8. Washington, M. T., Johnson, R. E., Prakash, S., and Prakash, L. (2000) Accuracy of thymine−thymine dimer bypass by *Saccharomyces cerevisiae* DNA polymerase η, *Proc. Natl. Acad. Sci. U.S.A. 97*, 3094−3099.
9. Sloane, D. L., Goodman, M. F., and Echols, H. (1988) The fidelity of base selection by the polymerase subunit of DNA polymerase III holoenzyme, *Nucleic Acids Res. 16*, 6465−6475.
10. Goodman, M. F. (1997) Hydrogen bonding revisted: Geometric selection as a principal determinant of DNA replication fidelity, *Proc. Natl. Acad. Sci. U.S.A. 94*, 10493−10495.
11. Kool, E. T. (2001) Hydrogen bonding, base stacking, and steric effects in DNA replication, *Annu. Rev. Biophys. Biomol. Struct. 30*, 1−22.
12. Kool, E. T. (2002) Active site tightness and substrate fit in DNA replication, *Annu. Rev. Biochem. 71*, 191−219.
13. Haracska, L., Washington, M. T., Prakash, S., and Prakash, L. (2001) Inefficient bypass of an abasic site by DNA polymerase η, *J. Biol. Chem. 276*, 6861−6866.
14. Berdis, A. J. (2001) Dynamics of translesion DNA synthesis catalyzed by the bacteriophage T4 exonuclease-deficient DNA polymerase, *Biochemistry 40*, 7180−7191.
15. Randall, S. K., Eritja, R., Kaplan, B. E., Petruska, J., and Goodman, M. F. (1987) Nucleotide insertion kinetics opposite abasic lesions in DNA, *J. Biol. Chem. 262*, 6864−6870.
16. Ide, H., Murayama, H., Sakamoto, S., Makino, K., Honda, K., Nakamuta, H., Sasali, M., and Sugimoto, N. (1995) On the mechanism of preferential incorporation of dAMP at abasic sites in translesional DNA synthesis. Role of proofreading activity of DNA polymerase and thermodynamic characterization of model template-primers containing an abasic site, *Nucleic Acids Res. 23*, 123−129.
17. Strauss, B. S. (1991) The "A rule" of mutagen specificity: A consequence of DNA polymerase bypass of non-instructional lesions? *Bioessays 13*, 79−84.
18. Taylor, J. S. (2002) New structural and mechanistic insight into the A-rule and the instructional and non-instructional behavior of DNA photoproducts and other lesions, *Mutat. Res. 510*, 55−70.
19. Matray, T. J., and Kool, E. T. (1999) A specific partner for abasic damage in DNA, *Nature 399*, 704−708.
20. Sun, L., Wang, M., Kool, E. T., and Taylor, J. S. (2000) Pyrene nucleotide as a mechanistic probe: Evidence for a transient abasic site-like intermediate in the bypass of dipyrimidine photoproducts by T7 DNA polymerase, *Biochemistry 39*, 14603−14610.
21. Sun, L., Zhang, K., Zhou, L., Hohler, P., Kool, E. T., Yuan, F., Wang, Z., and Taylor, J. S. (2003) Yeast pol η holds a *cis-syn* thymine dimer loosely in the active site during elongation opposite the 3′-T of the dimer, but tightly opposite the 5′-T, *Biochemistry 42*, 9431−9437.
22. Cannistraro, V. J., and Taylor, J. S. (2004) DNA−thumb interactions and processivity of T7 DNA polymerase in comparison to yeast polymerase η, *J. Biol. Chem. 279*, 18288−18295.
23. Taylor, J.-S., Brockie, I. R., and O'Day, C. L. (1987) A building block for the sequence-specific introduction of *cis-syn* thymine dimers into oligonucleotides. Solid-phase synthesis of TpT[*c*,*s*]-pTpT, *J. Am. Chem. Soc. 109*, 6735−6742.
24. Taylor, J.-S., and Nadji, S. (1991) Unraveling the origin of the major mutation induced by ultraviolet light, the C−T transition at dTpdC sites. A DNA synthesis building block for the *cis-syn* cyclobutane dimer of dTpdU, *Tetrahedron 47*, 2579−2590.
25. Ren, R. X. F., Chaudhuri, N. C., Paris, P. L., Rumney, S. I. V., and Kool, E. T. (1996) Naphthalene, phenanthrene, and pyrene as DNA base analogs: Synthesis, structure, and fluorescence in DNA, *J. Am. Chem. Soc. 118*, 7671−7678.
26. Shibutani, S., Takeshita, M., and Grollman, A. P. (1997) Translesional synthesis on DNA templates containing a single abasic site. A mechanistic study of the "A rule", *J. Biol. Chem. 272*, 13916−13922.
27. Bryant, F. R., Johnson, K. A., and Benkovic, S. J. (1983) Elementary steps in the DNA polymerase I reaction pathway, *Biochemistry 22*, 3537−3546.
28. Patel, S. S., Wong, I., and Johnson, K. A. (1991) Pre-steady-state kinetic analysis of processive DNA replication including complete characterization of an exonuclease-deficient mutant, *Biochemistry 30*, 511−525.
29. Washington, M. T., Prakash, L., and Prakash, S. (2001) Yeast DNA polymerase η utilizes an induced-fit mechanism of nucleotide incorporation, *Cell 107*, 917−927.
30. Washington, M. T., Wolfle, W. T., Spratt, T. E., Prakash, L., and Prakash, S. (2003) Yeast DNA polymerase η makes functional contacts with the DNA minor groove only at the incoming nucleoside triphosphate, *Proc. Natl. Acad. Sci. U.S.A. 100*, 5113−5118.
31. Petruska, J., and Goodman, M. F. (1985) Influence of neighboring bases on DNA polymerase insertion and proofreading fidelity, *J. Biol. Chem. 260*, 7533−7539.
32. Guckian, K. M., Schweitzer, B. A., Ren, R. X. F., Sheils, C. J., Tahmassebi, D. C., and Kool, E. T. (2000) Factors contributing to aromatic stacking in water: Evaluation in the context of DNA, *J. Am. Chem. Soc. 122*, 2213−2222.
33. Matray, T. J., and Kool, E. T. (1998) Selective and stable DNA base pairing without hydrogen bonds, *J. Am. Chem. Soc. 120*, 6191−6192.
34. Doublie, S., Tabor, S., Long, A. M., Richardson, C. C., and Ellenberger, T. (1998) Crystal structure of a bacteriophage T7 DNA replication complex at 2.2 Å resolution, *Nature 391*, 251−258.
35. Trincao, J., Johnson, R. E., Escalante, C. R., Prakash, S., Prakash, L., and Aggarwal, A. K. (2001) Structure of the catalytic core of *S. cerevisiae* DNA polymerase η: Implications for translesion DNA synthesis, *Mol. Cell 8*, 417−426.
36. Ling, H., Boudsocq, F., Plosky, B. S., Woodgate, R., and Yang, W. (2003) Replication of a *cis-syn* thymine dimer at atomic resolution, *Nature 424*, 1083−1087.
37. Washington, M. T., Helquist, S. A., Kool, E. T., Prakash, L., and Prakash, S. (2003) Requirement of Watson−Crick hydrogen bonding for DNA synthesis by yeast DNA polymerase η, *Mol. Cell. Biol. 23*, 5107−5112.
38. Bommarito, S., Peyret, N., and SantaLucia, J., Jr. (2000) Thermodynamic parameters for DNA sequences with dangling ends, *Nucleic Acids Res. 28*, 1929−1934.

39. Freier, S. M., Kierzek, R., Jaeger, J. A., Sugimoto, N., Caruthers, M. H., Neilson, T., and Turner, D. H. (1986) Improved free-energy parameters for predictions of RNA duplex stability, *Proc. Natl. Acad. Sci. U.S.A. 83*, 9373−9377.
40. Eom, S. H., Wang, J., and Steitz, T. A. (1996) Structure of Taq ploymerase with DNA at the polymerase active site, *Nature 382*, 278−281.
41. Pelletier, H., Sawaya, M. R., Kumar, A., Wilson, S. H., and Kraut, J. (1994) Structures of ternary complexes of rat DNA polymerase β, a DNA template-primer, and ddCTP, *Science 264*, 1891−1903.
42. Washington, M. T., Johnson, R. E., Prakash, S., and Prakash, L. (1999) Fidelity and processivity of *Saccharomyces cerevisiae* DNA polymerase η, *J. Biol. Chem. 274*, 36835−36838.
43. Huang, H., Chopra, R., Verdine, G. L., and Harrison, S. C. (1998) Structure of a covalently trapped catalytic complex of HIV-1 reverse transcriptase: Implications for drug resistance, *Science 282*, 1669−1675.
44. Kiefer, J. R., Mao, C., Braman, J. C., and Beese, L. S. (1998) Visualizing DNA replication in a catalytically active Bacillus DNA polymerase crystal, *Nature 391*, 304−307.
45. Smirnov, S., Matray, T. J., Kool, E. T., and de los Santos, C. (2002) Integrity of duplex structures without hydrogen bonding: DNA with pyrene paired at abasic sites, *Nucleic Acids Res. 30*, 5561−5569.

BI0489558